



Mechanical Design and Analysis of Eco-Print Textile Pounding Machine

Rhainna Rheizkhira Reflin^{1,2}, Steven Henderson Chang^{1,2}, Kushendarsyah Saptaji², Farid Triawan^{2,*}

¹Department of Aerospace and Mechanical Engineering, The University of Arizona, Tucson, AZ, 85721, USA

²Department of Mechanical Engineering, Faculty of Engineering and Technology, Sampoerna University, Jakarta Indonesia

*Correspondence: E-mail: farid.triawan@sampoernauniversity.ac.id

ABSTRACT

This study presents the design and analysis of an automated eco-print textile pounding machine to reduce labor intensity and preserve artistic aspects. The machine offers an efficient and cost-effective solution for businesses to meet the demand for eco-friendly textiles while maintaining control over the pounding technique. By utilizing a rotating flywheel mechanism, the device achieves approximately an average of 5 pounds with a force of 8.54 N per second. It features unique characteristics, including disassembly capability and replaceable parts for easy maintenance and longevity. The safety analysis indicates favorable safety factor values of 5.68 and 4.70 for static and dynamic loads, respectively, in the most critical part. Based on these results, it can be concluded that this product is safe and has a predicted infinite lifespan. This study serves as a valuable reference for the development of enhanced eco-print textile pounding machines.

ARTICLE INFO

Article History:

Submitted/Received 05 May 2023

First Revised 23 Jun 2023

Accepted 10 Aug 2023

First Available online 11 Aug 2023

Publication Date 01 Sep 2023

Keyword:

Automated machine,

Eco-print,

Rotating flywheel mechanism,

Safety analysis,

Textile pounding.

1. INTRODUCTION

The textile industry has played a vital role in human life for centuries, supplying fabrics for clothing, home decor, and various other products (Huang et al., 2021). In Indonesia, textile printing holds significant cultural value, with the traditional batik technique recognized as a UNESCO World Cultural Heritage (Poon, 2020; Widiawati & Arfan, 2020). Another traditional technique, known as the pounding technique or eco-pound printing, remains popular and adds cultural value to textiles (Nurmasitah & Sangadah, 2023).

Manual pounding, a labor-intensive process involving the application of dyes to fabric using a wooden mallet, requires a high level of skill and expertise (Yang et al., 2023). The consistency of pressure and rhythm during pounding is crucial to achieve desired patterns and designs (Wang et al., 2021). Despite the skill required, manual pounding continues to be extensively employed in Indonesia, particularly within the souvenir industry, where there is a high demand for unique and sustainable textile products (Rahayuningsih et al., 2022).

With the rise in demand for environmentally friendly items, there is a growing market for sustainable textile products in the souvenir industry, contributing significantly to the Indonesian economy (Meitiana et al., 2019; Chen et al., 2021). However, the manual pounding method is time-consuming and labor-intensive, making it difficult for small and medium-sized businesses to meet the growing demand for eco-friendly textiles (Bureekhampun & Maneepun, 2021). Consequently, there is a need for a more efficient and cost-effective approach to applying colors to fabrics using a unique eco-pounding technique.

This study focuses on designing an automated and economical machine for the pounding technique, addressing the need for an efficient and cost-effective method while maintaining the unique motive of eco-pounding dye application in the souvenir industry. This study was also supported by mathematical analysis and several terms are explained in **Table 1**.

Table 1. Nomenclature.

Term	Description
F_{spring}	Force exerted by Spring (N)
k	Spring Constant (N/m)
d_1	Displacement from the Origin Point (m)
G	Shear Modulus (N/mm ²)
d_2	Wire Diameter of the Spring (mm)
D	Mean Coil Diameter of the Spring (mm)
n	Number of Active Coils in Spring
F_{impact}	Final Force with Impact Effect (N)
M	System Mass (kg)
v	Final Impact Velocity (m/s)
T	Applied Torque (Nm)
F	Applied Force (N)
r	Radius (m)
M	Applied Moment (Nm)
S'_e	Ideal Endurance Strength (MPa)
S_e	Endurance Strength (MPa)
S_{ut}	Ultimate Strength (MPa)
k_a	Surface Condition Modification Factor
k_b	Size Modification Factor
k_c	Load Modification Factor
k_d	Temperature Modification Factor
k_e	Reliability Factor
k_f	Miscellaneous-Effects Modification Factor

Table 1 (continue). Nomenclature.

Term	Description
K_f	Fatigue Stress-Concentration Factor
K_{fs}	Static Stress-Concentration Factor
σ'_a, σ'_m	Von Mises Stresses (MPa)
σ_a	Alternate Stress (MPa)
σ_m	Mid-range Stress (MPa)
τ_m	Mid-range Shear Stress (MPa)
F_{key}	Reaction Force of Key (N)
A_{key}	Surface Area of Key (m ²)
M_a	Alternate Moment (Nm)
T_a	Alternate Torque (Nm)
M_m	Mid-range Moment (Nm)
T_m	Mid-range Torque (Nm)
d	Diameter (m)
S_y	Yield Strength (MPa)
n_y	Static Factor of Safety
n_f	Dynamic or Fatigue Factor of Safety

By automating the process, this machine eliminates manual work, resulting in a more productive and less labor-intensive approach (Coombs *et al.*, 2020). Its key feature is replaceable mallet and hammerheads, providing flexibility and customization for fabric decoration to meet the diverse needs of the textile industry.

The target market for this innovative machine includes small and medium-sized businesses in the souvenir industry, providing them with a user-friendly and cost-effective solution to meet the rising demand for eco-friendly products. By adopting this automated machine, businesses can effectively address resource constraints while maintaining product quality. Furthermore, the machine contributes to sustainability efforts by enabling the production of unique and environmentally friendly textile products.

As of now, no existing patent or paper reports a similar machine, making this study a pioneering solution in the field of textile printing. Its uniqueness and potential impact add significance to the development of an automated machine for eco-pounding printing in the Indonesian textile industry. This advancement has the potential to revolutionize the traditional pounding technique, reduce manual labor, and preserve cultural heritage without compromising quality.

Overall, the development of an automated machine for eco-pounding printing in the Indonesian textile industry presents an opportunity to revolutionize the traditional pounding technique, reduce manual labor, and promote sustainable and distinctive textile products. This innovative solution empowers businesses to meet market demands while preserving cultural heritage.

2. METHODS

The design process follows the design flowchart outlined in **Figure 1**, conducted in stages. It was repeated as necessary until the desired results were achieved. SolidWorks 2020 CAD software was used to model the design, providing accurate and detailed design models (Panchenko, 2023). Additionally, the software enables strength analysis and problem-solving before manufacturing. By adhering to this design process, the resulting design is expected to meet all requirements and user needs effectively and efficiently.



Figure 1. Design process.

2.1. Problem Definition and Specification

The manual hand-pounding technique used in eco-printing poses physical challenges for laborers, leading to arm fatigue and limiting production rates. To address these concerns, an automated machine is required to alleviate the workload while preserving the uniqueness of the pounding technique. The machine should also offer improved control over texture and coloring through the use of replaceable hammerheads.

The primary specifications for the machine are rapid pounding and strong force. It should achieve an average frequency of 5 pounds per second to increase production rates while maintaining the uniqueness of the technique. The machine should exert a stress of at least 50 kPa to ensure high-quality printing results. The estimated force exerted during pounding is around 10 Newtons (N), which yields an estimated stress of 50 kPa when distributed over a 2 cm² area. However, the actual stress may vary depending on factors such as leaf size, hammer type, and pounding strength.

The secondary specifications are an economical price and small size. The machine should be priced under Rp 5 million and have less than 50 × 50 × 50 cm³ dimensions for affordability, accessibility, and portability. An adjustable pounding speed ranging from 3 to 7 poundings per second should be included to accommodate different material densities and hardness levels, ensuring versatility in its use.

Lastly, the tertiary specification is that the machine should augment rather than replace the artistic aspect of eco-printing. Human intervention and creativity are still required to arrange patterns and control the pounding area. While automated features may be included, the machine should serve as a tool to aid artists and not replace their creative abilities.

By adhering to these specifications, the aim is to create a machine that meets the needs of artists in terms of ease of use, productivity, affordability, and versatility while preserving the cultural and artistic aspects of eco-printing.

2.2. Design Concept

The design concept of the Eco-Print Textile Pounding Machine, illustrated in **Figure 2**, focuses on achieving efficient and eco-friendly pigment transfer to create intricate patterns on fabric or paper. This compact and economical machine incorporates various mechanisms and components to optimize performance and ensure user safety. The machine is designed to deliver optimal performance with a durable thermoplastic polyester frame, an adjustable-speed motor capable of reaching 300 RPM, a spring mechanism, a replaceable pounder made of hardened steel, and a size of approximately 25x15x26 cm³. This section provides a detailed analysis and description of the design concept, outlining the functionality and significance of each key component.

The operation of the machine involves several key elements. Firstly, the eco-material to be pounded is positioned beneath the pounder rod, which is covered by fabric or paper for pattern transfer. The rotational motion and torque required for pounding are transmitted from the motor to the main connector shaft through the shaft coupler. The main connector shaft, aided by a key, transfers this motion to the flywheel-shaped disk. As the disk rotates counterclockwise, it elevates the up-and-down pounder mechanism using the small connector rod and wheel. The up-and-down pounder mechanism consists of a pounder rod that effectively pounds the eco-material. A spring on the output rod, working in conjunction with gravity and free fall, delivers a powerful force to pulverize the eco-material into small particles. Additionally, the spring helps maintain a constant connection between the wheel and the disk. The output rod and pounder rod are securely connected to the connector using bolts and nuts to ensure stability.

The machine allows for adjustable pounding speed by controlling the motor speed, with fine control provided by a Pulse Width Modulation (PWM) controller. The use of replaceable parts, such as keys and pounder rods, facilitates easy maintenance and enhances the longevity of the machine. The pounding rate can be controlled by replacing the wheels. Safety features are incorporated, including a movable connector that can temporarily halt the pounder rod by disconnecting the wheel and disk, prioritizing operator safety.

In terms of power requirements, the design is based on the comparison of the Freelab DC Motor GA12 N20 product, which operates at a 12 Volt DC working voltage to achieve the desired speed of 300 RPM. This choice of motor ensures affordability and accessibility for small-scale businesses. By utilizing a 12 Volt DC motor, which is cost-effective and lightweight, the design meets the needs of small-scale textile production enterprises. Based on the comparison, the machine only requires a 12 Volt DC working voltage to perform 300 pounds per minute, which is suitable for small-scale textile production by micro, small, and medium enterprises (MSMEs). Achieving a pounding frequency of approximately 5 pounds per second can be accomplished by applying a torque of 0.4 Nm to the pounder mechanism.

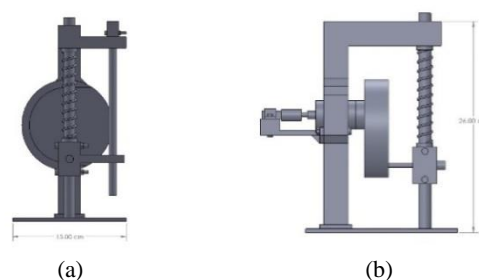


Figure 2. Proposed machine design view: (a) Front, (b) Side, (c) Top, and (d) Isometric.

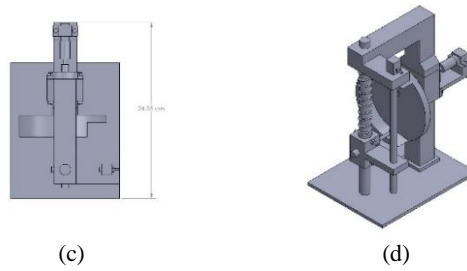


Figure 2 (continue). Proposed machine design view: (a) Front, (b) Side, (c) Top, and (d) Isometric.

2.3 Manufacturing Process

The Eco-Print Textile Pounding Machine consists of various components that collectively contribute to its final design. To enhance comprehension of each component type, an exploded view of the machine's final design is provided in **Figure 3**.

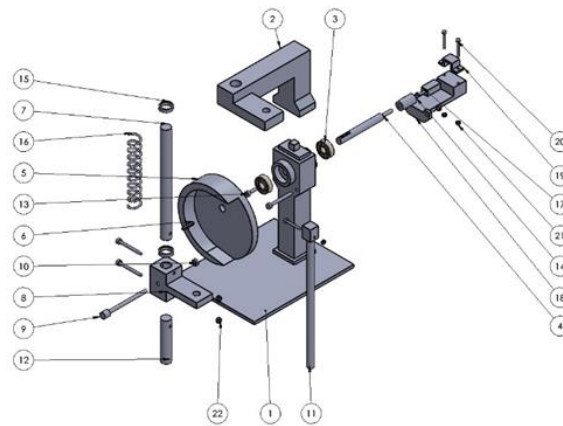


Figure 3. Exploded view of machine design.

To meet product specifications and ensure long-term performance, careful selection of materials for the eco-pounding machine is essential, considering their impact on the product's life cycle (Vanova et al., 2021). Consequently, carbon steel S45C, stainless steel 304, and polylactic acid (PLA) were chosen as the primary materials for manufacturing. Each material was selected based on its specific properties: S45C for its strength and toughness, stainless steel 304 for its corrosion resistance and durability, and PLA for its eco-friendliness and cost-effectiveness (Wang et al., 2023). These material choices ensure that the machine components not only meet the necessary criteria but also deliver optimal performance in their respective applications. The materials and manufacturing methods employed for the components of the automated eco-pounding machine's final design are depicted in **Figure 2** and **Figure 3** and are detailed in **Table 1**.

2.4. Analysis Procedure

The analysis procedure for the design and analysis of the eco-print textile pounding machine involves sequential steps (Khoiriyah et al., 2021; Hadisujoto and Wijaya, 2021). It starts with a Free Body Diagram (FBD) static equilibrium analysis to determine forces, stresses, and strains on critical components. Von Mises stress analysis predicts failure under complex loading, while fatigue analysis assesses durability considering stress amplitude and mean stress. Static and fatigue safety factor analysis ensures compliance with safety and reliability standards. The procedure incorporates Hooke's Law for spring force and calculates

the maximum equivalent impact force using kinetic energy (Xue et al., 2022). The following equations (1-10) were utilized in this analysis. This comprehensive procedure ensures the strength and reliability of the eco-print textile pounding machine.

Table 1. List of components for machine design.

No.	Component's Name	Material	Method
1	Base Frame	PLA	3D Printing
2	Upper Frame	PLA	3D Printing
3	6000ZZ Ball Bearing	SS304	Standardized
4	Main Connector Shaft	S45C	Milling
5	Disk	PLA	3D Printing
6	Key	PLA	3D Printing
7	Output Rod	S45C	Drill Press
8	Connector	PLA	3D Printing
9	Small Connector Rod		Standardized
10	Wheel	Ball Bearing	Standardized
11	Stabiliser Rod	S45C	Standardized
12	Pounder Rod	S45C	Drill Press
13	M4 Bolt	SS304	Standardized
14	Shaft Coupler	Aluminum Alloy	Standardized
15	Spring Plate	S45C	Milling
16	Spring	Steel	Standardized
17	DC Motor GA12 N20	Metal + Copper	Standardized
18	Motor Support	PLA	3D Printing
19	Motor Bracket	PLA	3D Printing
20	M3 Bolt	SS304	Standardized
21	M3 Nut	SS304	Standardized

$$F_{spring} = kd_1 \tag{1}$$

$$k = \frac{Gd_2^4}{8D^3n} \tag{2}$$

$$F_{impact} = \frac{mv^2}{d_1} \tag{3}$$

$$T = Fr \tag{4}$$

$$M = Fd_2 \tag{5}$$

$$\sum F_x(\rightarrow +) = 0 \tag{6}$$

$$\sum F_y(\uparrow +) = 0 \tag{7}$$

$$\sum M(\curvearrowright +) = 0 \tag{8}$$

$$\sum T(\curvearrowright +) = 0 \tag{9}$$

$$S_e = k_a k_b k_c k_d k_e k_f S'_e \tag{10}$$

The analysis procedure for determining the ideal endurance strength S'_e and the Marin Factors, as required to solve Equation 10, involves utilizing the formulas provided in Shigley's book (equation 11-21). **Table 2** and **Figure 4** assist in estimating stress concentration factors during stress analysis, while **Figure 5** and **Figure 6** support the estimation of notch sensitivities.

Table 2. Stress concentration factors (kt and kts) estimation.

	Bending	Torsional	Axial
Shoulder fillet–sharp (r/d = 0.02)	2.7	2.2	3.0
Shoulder fillet–well rounded (r/d = 0.1)	1.7	1.5	1.9
End-mill keyseat	2.14	3.0	–
Sled runner keyseat	1.7	–	–
Retaining ring groove	5.0	3.0	5.0

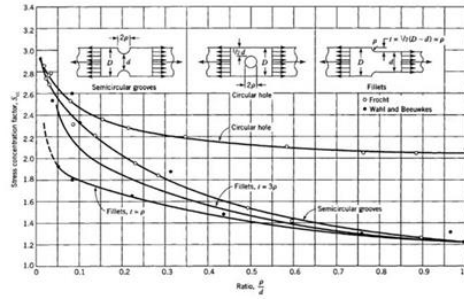


Figure 1. Stress concentration factor for solid shaft with transverse hole with axial load.

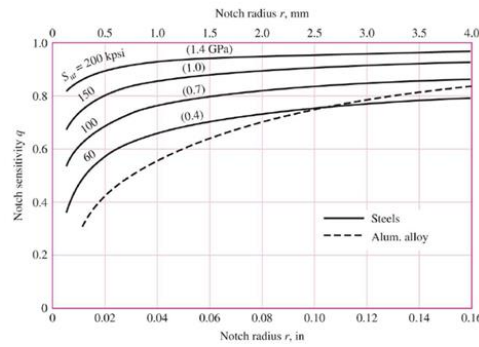


Figure 5. Notch sensitivity (q) chart.

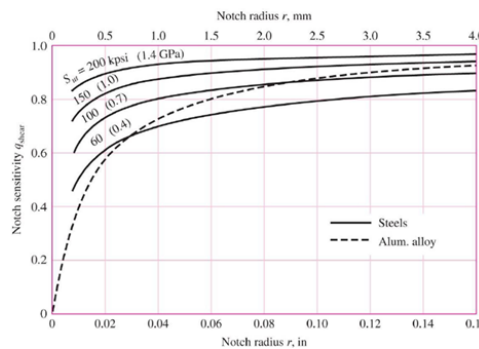


Figure 6. Notch sensitivity for shear (q_{shear}) chart.

$$K_f = 1 + q(K_t - 1) \tag{11}$$

$$K_{fs} = 1 + q_{shear}(K_{ts} - 1) \tag{12}$$

$$\sigma'_a = \sqrt{\sigma_a^2 + \tau_a^2} = \sqrt{\left(\frac{32K_f M_a}{\pi d^3}\right)^2 + 3\left(\frac{16K_{fs} T_a}{\pi d^3}\right)^2} \tag{13}$$

$$\sigma'_m = \sqrt{\sigma_m^2 + \tau_m^2} = \sqrt{\left(\frac{32K_f M_m}{\pi d^3}\right)^2 + 3\left(\frac{16K_{fs} T_m}{\pi d^3}\right)^2} \tag{14}$$

$$\tau'_m = \frac{V}{A} = \frac{F_{key}}{A_{key}} \tag{15}$$

$$n_y = \frac{S_y}{\sigma'_{max}} = \frac{S_y}{(\sigma'_a + \sigma'_m)} \quad (16)$$

$$A = \sqrt{4(K_f M_a)^2 + 3(K_{fs} T_a)^2} \quad (17)$$

$$B = \sqrt{4(K_f M_m)^2 + 3(K_{fs} T_m)^2} \quad (18)$$

$$\frac{1}{n_{f,DE-GERBER}} = \frac{8A}{\pi d^3 S_e} \left(1 + \sqrt{1 + \left(\frac{2BS_e}{AS_{ut}} \right)^2} \right) \quad (19)$$

$$\frac{1}{n_{f,DE-Soderberg}} = \frac{16}{\pi d^3} \left(\frac{1}{S_e} \sqrt{4(K_f M_a)^2 + 3(K_{fs} T_a)^2} + \right. \quad (20)$$

$$\left. \frac{1}{S_y} \sqrt{4(K_f M_m)^2 + 3(K_{fs} T_m)^2} \right)$$

$$\frac{1}{n_{f,Soderberg}} = \frac{\sigma_a}{S_e} + \frac{\sigma_m}{S_y} \quad (21)$$

3. RESULTS AND DISCUSSION

The prototype of the eco-print textile pounding machine, developed for demonstration purposes, closely resembles the original 3D design with minimal modifications. It has successfully achieved its intended functionality and operation. A visual representation of the prototype and its outcome is provided in **Figure 7**.



Figure 7. Isometric view of machine prototype based on the design.

The design of the eco-print textile pounding machine also undergoes comprehensive analysis, including loading, stress, fatigue condition, and safety analysis during the analysis and optimization stage. Four components, namely the main connector shaft, key, small connector rod, and pounder rod, are subjected to analysis. The resulting data from this stage is presented in this section.

3.1. Analysis Assumption

The analysis of the eco-print textile pounding machine incorporates several assumptions to facilitate the calculation process and other considerations. These assumptions are as follows:

- (i) Other components (frame, disk, etc.) within the machine are not analyzed as they are assumed to be non-critical, safe, and have a predicted infinite lifespan.
- (ii) The effect of impact resulting from the contact of the pouncer during the pounding process is considered and its estimation is included in the force calculation as F_{impact} .

3.2. Force, Moment, and Torque Analysis

The critical component analysis starts with free-body diagrams, calculated using Equations 1 and 3 to 9. **Figure 8** displays the diagram and loading values for the main connector shaft, while **Figure 9** illustrates the shear force experienced by the key component due to applied torque. **Figure 10** demonstrates the force representation for the small connector rod, considering its small size. Lastly, **Figure 11** presents the free-body diagram of the pouncer rod. All component dimensions are provided in **Figure 12**.

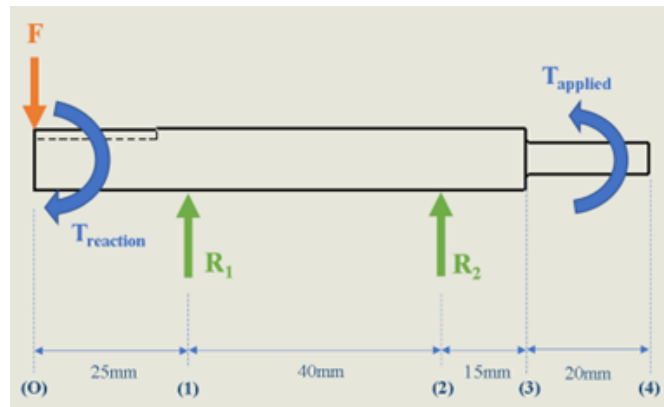


Figure 2. Free-body diagram of main connector shaft.

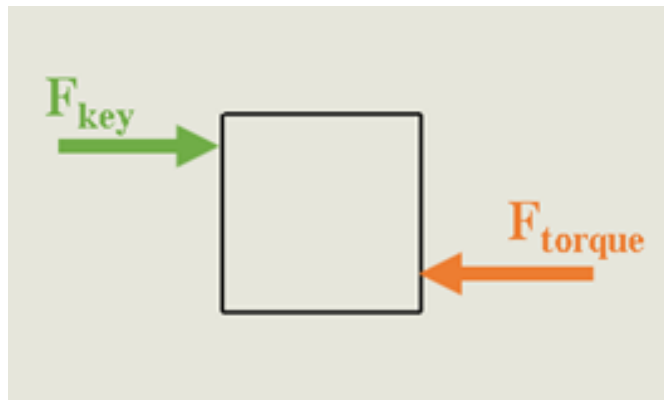


Figure 9. Free-body diagram of shaft key.

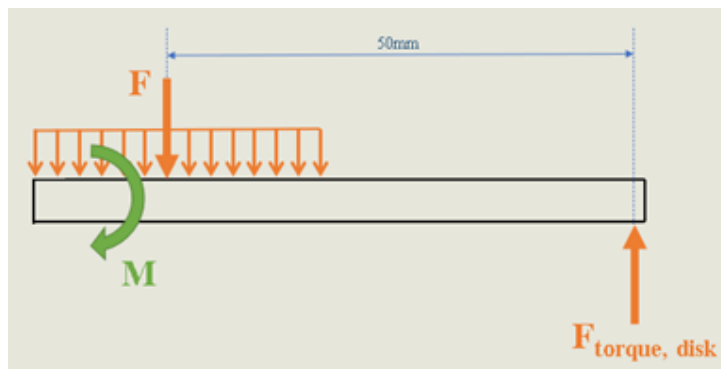


Figure 10. Free-body diagram of small connector rod.

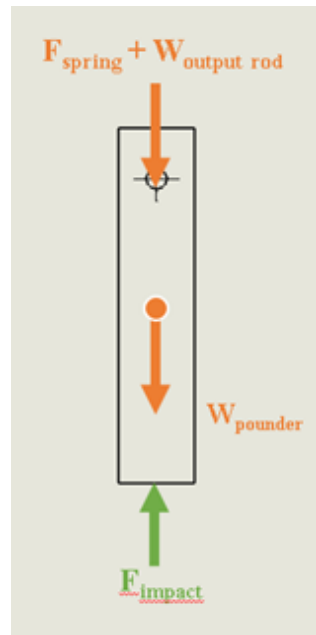


Figure 11. Free-body diagram of pounder rod.

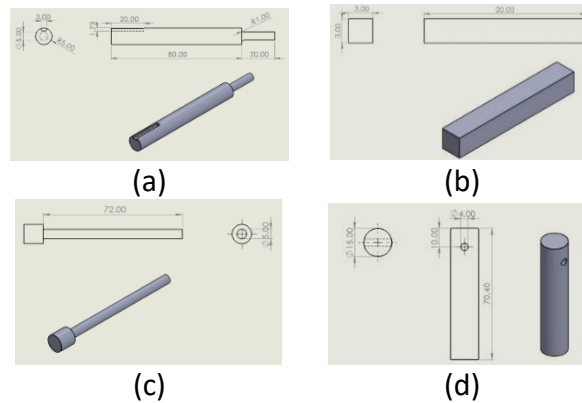


Figure 3. Dimensions: (a) Main connector shaft, (b) Key, (c) Small connector rod, and (d) Pounder rod.

Before conducting the analysis, certain forces are predetermined. The spring force is determined using Equation 2, while the torque is obtained from the given specification of the rated torque from the motor used. The calculated values from the free-body diagram analysis are presented in **Table 3**.

Table 1. Force, moment, and torque values of the components.

Parameter name	Value
F	5.133 N
R_1	8.340 N
R_2	-3.210 N
$T_{applied}$	0.392 Nm
$T_{reaction}$	-0.392 Nm
F_{torque}	78.400 N
F_{key}	-78.400 N
M	0.600 Nm
$F_{torque,disk}$	11.910 N
F_{spring}	1.725 N
$W_{output rod}$	2.450 N

Table 2 (continue). Force, moment, and torque values of the components.

Parameter name	Value
$W_{pounder}$	0.960 N
F_{impact}	8.540 N

The previously found shear force and moment values from the free-body diagrams, along with the moment calculation using Equations 6 to 7, are considered in these diagrams. **Figure 13** and **Figure 14** display these diagrams for the main connector shaft, while **Figure 15** and **Figure 16** present the corresponding diagrams for the small connector rod.

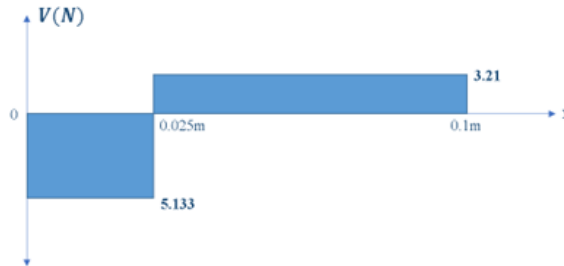


Figure 13. Shear force diagram of main connector shaft.

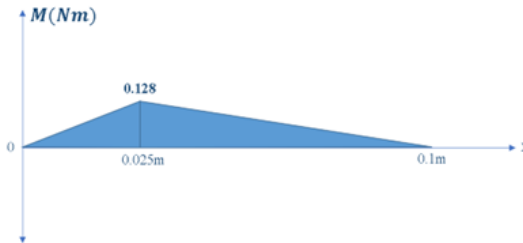


Figure 14. Bending moment diagram of main connector shaft.

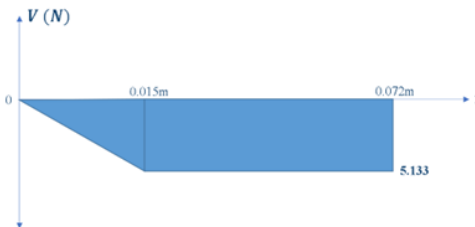


Figure 15. Shear force diagram of small connector rod.

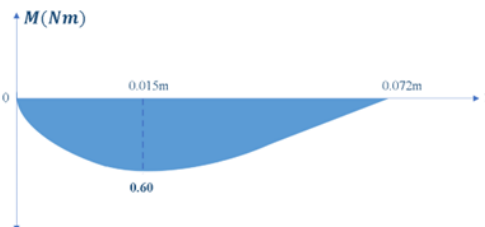


Figure 16. Bending moment diagram of small connector rod.

Based on the bending moment and shear force diagrams, it is evident that the most critical loading occurs at a specific point along the components. For the main connector shaft, the most critical point is located at support bearing 1, 0.025 m from the left end. Likewise, the connector rod's critical loading is at a position 0.015 m from the left end. These points will be the primary focus of the safety analysis for the respective components.

3.3. Stress Analysis

The analysis of components with notches, holes, or shoulder fillets involves determining stress concentration factors using Equations 11 and 12, along with the aid of approximation charts in **Figures 4 to 6** and estimations from **Table 2**. Components without stress concentration are denoted by a dash (-) in **Tables 4, 5, and 6**, which provides the notch sensitivity and stress concentration factors for each component. These values will also be used in the fatigue analysis.

Table 4. Notch sensitivity.

Components	Notch sensitivity	
	q	q _s
Main Connector Shaft	0.55	0.56
Pounder Rod	0.80	-

Table 5. Stress concentration factors.

Components	Stress concentration factors			
	K _t	K _{ts}	K _f	K _{fs}
Main Connector Shaft	2.14	3	1.627	2.12
Pounder Rod	2.24	1	1.992	1.00

Once the stress concentration factors are determined, the calculation of midrange and alternating stresses can be performed using Equations 13 to 15. The key component experiences shear stress, while the small connector rod and pounder rod exhibit normal stresses. It should be noted that no alternating shear stresses are applied to any of the components. **Table 7** presents the calculated midrange and alternating stresses for each component.

Table 6. Mid-range and alternating stress of components.

Components	σ_m (MPa)	σ_a (MPa)	τ_m (MPa)
Main Connector Shaft	7.407	1.061	-
Key	-	-	1.307
Small Connector Rod	24.310	24.310	-
Pounder Rod	0.146	0.146	-

3.4. Static Analysis

The static analysis of the components, utilizing Equation 15 and the previously obtained values, results in the calculation of safety factor values presented in **Table 7**. Notably, all analyzed components demonstrate a static factor of safety exceeding 1, indicating their ability to withstand the applied loads without failure or excessive deformation (Peng et al., 2022). This ensures reliable performance within acceptable limits.

Table 7. Static safety factors.

Components	Static Safety Factor
Main Connector Shaft	62.59
Key	19.70
Small Connector Rod	5.68
Pounder Rod	1818.09

3.4. Fatigue Analysis

In the fatigue analysis, the determination of Marin Factors using Equation 10 is the first step. However, the component key is not subjected to cyclic loading and is therefore excluded from the Marin factor analysis. The Marin factors for each component, along with the modified values of the endurance strength, are presented in **Table 8** and **Table 9**.

Table 8. Marin factors.

Components	Marin Factors			
	k_a	k_b	k_c	k_e
Main Connector Shaft	0.82	0.97	1.00	0.62
Key	-	-	-	-
Small Connector Rod	0.84	1.04	1.00	0.62
Pounder Rod	0.82	1.00	0.85	0.62

Table 9. Endurance strength.

Components	S'_e (MPa)	S_e (MPa)
Main Connector Shaft	315	154.7
Key	-	-
Small Connector Rod	284	154.4
Pounder Rod	315	135.7

Based on the subsequent calculations using the previously obtained values, the fatigue analysis of the components reveals the safety factors using Equations 19 to 20. The results, presented in **Table 10**, demonstrate that all analyzed components possess a fatigue factor of safety exceeding 1. This signifies that the components are able to withstand cyclic loading and fatigue conditions, ensuring their reliable performance and longevity within acceptable limits (Farhat & Salvini, 2022).

Table 10. Fatigue safety factors.

Components	Fatigue Safety Factor	
	DE-Soderberg	DE-Gerber
Main Connector Shaft	48.00	63.80
Key	-	-
Small Connector Rod	4.07	5.94
Pounder Rod	741.10	891.20

The comprehensive analysis conducted on the components of the Eco-Print Textile Pounding Machine reveals promising results in terms of safety and performance. All components exhibit safety factors above 1, ensuring their ability to withstand static and cyclic loading. Remarkably, the fatigue safety factors suggest an infinite lifespan for the fatigue-exposed components. The design choices are evident in the varying safety factors, with the main connector shaft prioritized for robustness as the primary motion transmitter. The small connector rod demonstrates a lower safety factor due to its smaller dimensions and material characteristics. On the other hand, the pounder rod boasts the highest safety factor, owing to deliberate decisions regarding material selection and force specifications. The decisions for the pounder rod were made to enable practical and affordable manufacturing while contributing to the pounding force. These findings affirm the practical and cost-effective manufacturing approach while maintaining optimal pounding force capabilities.

4. CONCLUSION

In summary, this study introduces an automated eco-print textile pounding machine that efficiently reduces labor intensity while preserving artistic aspects in textile production. The machine, powered by a DC motor with a rotating flywheel mechanism, achieves a pounding rate of approximately 5 pounds per second, applying 8.54 N of force to enable vertical motion of the pounder rod. Comprehensive strength analysis reveals the machine's ability to withstand loads under various conditions, ensuring its safety and durability. Disassembly capability and replaceable parts facilitate easy maintenance, while fatigue analysis supports its robustness.

However, to enhance functionality, motor upgrading is recommended for independent flywheel rotation, with moment of inertia calculations for motor selection. Addressing vibration issues by exploring dampeners or a steel base is crucial, and securing the machine to a table can prevent movement, ensuring optimal performance. These findings offer valuable insights into design considerations, safety analysis, and performance optimization for eco-print textile pounding machines.

5. ACKNOWLEDGMENT

This study is supported by the Faculty of Engineering and Technology (FET) and the Center for Research and Community Service (CRCS), at Sampoerna University, Indonesia.

6. AUTHORS' NOTE

The authors declare that there is no conflict of interest regarding the publication of this article. Authors confirmed that the paper was free of plagiarism.

7. REFERENCES

- Bureekhampun, S., and Maneepun, C. (2021). Eco-friendly and community sustainable textile fabric dyeing methods from Thai buffalo manure: From pasture to fashion designer. *SAGE Open*, 11(4), 1-13.
- Chen, X., Memon, H. A., Wang, Y., Marriam, I., and Tebyetekerwa, M. (2021). Circular economy and sustainability of the clothing and textile industry. *Materials Circular Economy*, 3(12), 1-9.
- Coombs, C., Hislop, D., Taneva, S. K., and Barnard, S. (2020). The strategic impacts of intelligent automation for knowledge and service work: An interdisciplinary review. *The Journal of Strategic Information Systems*, 29(4), 1-30.
- Farhat, H., and Salvini, C. (2022). Novel gas turbine challenges to support the clean energy transition. *Energies*, 15(15), 1-17.
- Hadisujoto, B., and Wijaya, R. (2021). Development and accuracy test of a fused deposition modeling (FDM) 3D printing using H-Bot mechanism. *Indonesian Journal of Computing, Engineering and Design (IJoCED)*, 3(1), 46-53.
- Huang, R., Yan, P., and Yang, X. (2021). Knowledge map visualization of technology hotspots and development trends in China's textile manufacturing industry. *IET Collaborative Intelligent Manufacturing*, 3(3), 243-251.

- Khoiriyah, N., Alfatih, S. A., Munir, M., and Triawan, F. (2021). Component design and strength analysis of coffin lowering machine for Covid-19 corpse: A problem-based learning. *Indonesian Journal of Multidisciplinary Research*, 1(1), 137-150.
- Meitiana, M., Setiawan, M., Rohman, F., and Irawanto, D. W. (2019). Factors affecting souvenir purchase behavior: valuable insight for tourism marketers and industry. *Journal of Business and Retail Management Research*, 13(3), 248-255.
- Nurmasitah, S., and Sangadah, S. F. (2023). The quality of Jatropha leaf ecoprint products using steaming and pounding techniques. *In IOP Conference Series: Earth and Environmental Science*, 1203(1), 012020.
- Panchenko, O. (2023). Assessing the accuracy of modeling the tubbing erector manipulator mechanism in solidworks motion program. *Natsional'nyi Hirnychiy Universytet. Naukovyi Visnyk*, 2023(3), 75-80.
- Peng, J., Hou, C., and Shen, L. (2022). Progressive collapse analysis of corner-supported composite modular buildings. *Journal of Building Engineering*, 48, 103977.
- Poon, S. (2020). Symbolic resistance: tradition in batik transitions sustain beauty, cultural heritage and status in the era of modernity. *World Journal of Social Science*, 7(2), 1-10.
- Rahayuningsih, E., Marfitania, T., Pamungkas, M. S., and Fatimah, W. S. (2022). Optimization of cotton fabrics dyeing process using various natural dye extracts. *Jurnal Rekayasa Proses*, 16(1), 58-65.
- Vanova, R., Igaz, R., Nemec, M., Stefkova, J., and Stefko, J. (2021). A Passive wood-based building in slovakia: Exploring the life cycle impact. *Forests*, 12(12), 1-23.
- Wang, Q., Zhang, G., Zheng, X., Ni, Y., Liu, F., Liu, Y., and Xu, L. R. (2023). Efficient characterization on the interlayer shear strengths of 3D printing polymers. *Journal of Materials Research and Technology*, 22, 2768-2780.
- Wang, Y. W., Yi, Q. Z., Ding, Y., Ji, F., and Wang, N. (2021). Study on the factors influencing the dyeing performance of cotton fabric with vat dyes based on principal component analysis. *The Journal of the Textile Institute*, 112(9), 1460-1466.
- Widiawati, D., and Arfan, N. (2020). Utilization of local resources for batik design development in Indonesia textile industry. *PalArch's Journal of Archaeology of Egypt/Egyptology*, 17(4), 1609-1627.
- Xue, L., Li, H., Li, A., Zhao, Z., Li, K., Li, M., and Song, Y. (2022). Non-hookean droplet spring for enhancing hydropower harvest. *Small*, 18(18), 2200875.
- Yang, R., Pei, S., Xie, Y., Yan, X., Inta, A., and Yang, L. (2023). Ethnobotanical research on dye plants used by the baiyi indigenous peoples' from Heqing County, Dali, Yunnan, China. *Diversity*, 15(7), 856.